New Journal of Physics
The open access journal at the forefront of physics
Deutsche Physikalische Gesellschaft DPG | IOP Institute of Physics

Synchronization in networks of mutually delay-coupled phase-locked loops

Alexandros Pollakis[1,3], Lucas Wetzel[2,3], David J Jörg[2,3], Wolfgang Rave[1,3], Gerhard Fettweis[1,3] and Frank Jülicher[2,3]

[1] Technische Universität Dresden, Vodafone Chair, Dresden, Germany
[2] Max Planck Institute for the Physics of Complex Systems, Dresden, Germany
[3] Center for Advancing Electronics Dresden cfAED, Dresden, Germany
E-mail: Gerhard.Fettweis@vodafone-chair.com and julicher@pks.mpg.de

Received 9 July 2014, revised 10 September 2014
Accepted for publication 18 September 2014
Published 4 November 2014
New Journal of Physics **16** (2014) 113009
doi:10.1088/1367-2630/16/11/113009

Abstract

Electronic components that perform tasks in a concerted way rely on a common time reference. For instance, parallel computing demands synchronous clocking of multiple cores or processors to reliably carry out joint computations. Here, we show that mutually coupled phase-locked loops (PLLs) enable synchronous clocking in large-scale systems with transmission delays. We present a phase description of coupled PLLs that includes filter kernels and delayed signal transmission. We find that transmission delays in the coupling enable the existence of stable synchronized states, while instantaneously coupled PLLs do not tend to synchronize. We show how filtering and transmission delays govern the collective frequency and the time scale of synchronization.

Keywords: phase-locked loops, transmission delay, synchronization, mutual coupling, filtering

1. Introduction

Parallel information processing has become more and more important in modern electronics. Prominent examples are multi-processor and multi-core computer architectures, network-on-

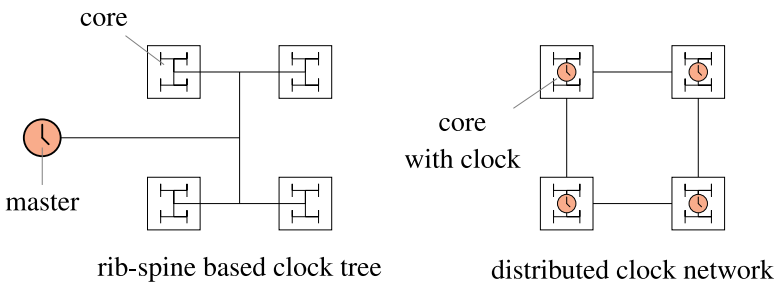

Figure 1. Concepts for clock distribution in spatially extended networks. Left: traditional concept using one master clock as reference and equally long wires towards each core. Right: alternative concept of a clocking network with mutually coupled nodes.

chips, mobile communication systems, and antenna arrays [1–4]. Parallel processing requires coordination of the different components. In multi-core systems, for instance, the trend to integrate more and more processing cores in a single silicon die is driven by benefits in computational performance, energy and cost efficiency. Such systems may consist of tens to hundreds of cores. One important strategy to coordinate the components is to provide a common time reference using clocking devices. Global coordination can be achieved using a master-clock design, where one master clock synchronizes different cores via a so-called clock tree using phase-locked loops (figure 1). A phase-locked loop (PLL) generates a clock signal controlled by an external master clock using internal feedback [5, 6]. This clocking design is efficient for small systems but becomes space and energy inefficient as system size increases [7, 8]. Therefore, the standard method to provide clocking for large systems with many cores is the so-called globally asynchronous locally synchronous (GALS) clocking [9]. In this approach, only local subgroups of components are in synchrony, while communication between asynchronous subgroups requires waiting cycles to guarantee proper parallel processing. Therefore, this approach leads to performance loss due to communication latencies between domains with different time references [10, 11]. For these reasons, it is important to find alternative clocking designs that are optimized to function in large systems.

In principle, global coordination of many components could be achieved by self-organized synchronization via mutual coupling. Such an approach does not rely on a master clock and is thus expected to be scalable [12–14]. At high clock rates of several gigahertz which are common in modern electronics, significant transmission delays arise on the centimeter scale and influence the system behavior. This raises the question which system architectures are needed to obtain global synchrony in large systems and whether transmission delays pose an extra challenge.

In this paper, we derive a phase model for a network of mutually coupled phase-locked loops with transmission delays but without a master clock (figure 1). In section 2, we give a brief introduction to PLLs and derive a phase model for N delay-coupled PLLs with arbitrary coupling topology. In section 3, the synchronized state is investigated, followed by a linear stability analysis in section 4. In section 5, we illustrate our results using specific examples and conclude the work with a discussion in section 6.

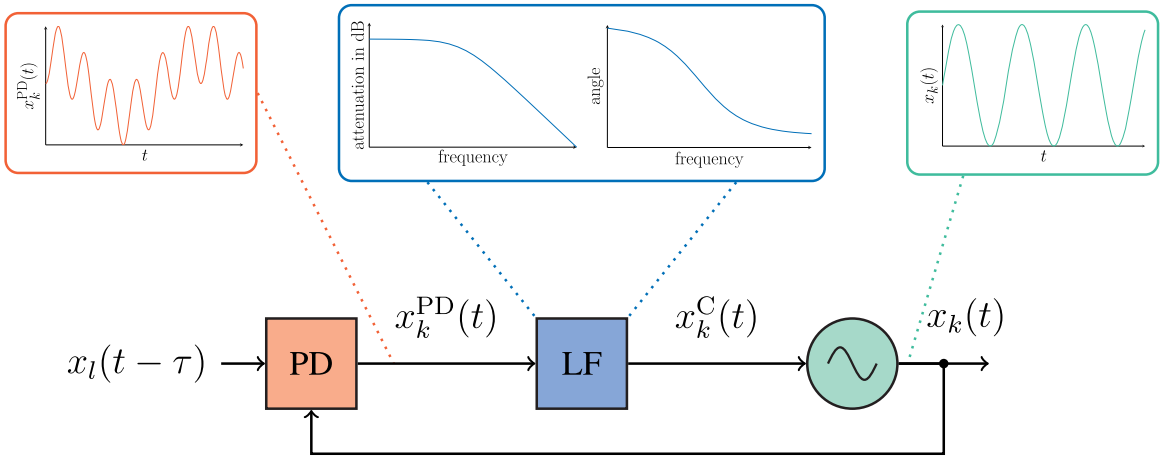

Figure 2. Signal flow of a PLL. The input signal to PLL k is denoted by $x_l(t)$ and its output signal by $x_k(t)$. The output signal $x_k(t)$ is generated by a voltage-controlled oscillator (VCO, green). The output signal at the phase detector (PD, red) is denoted by $x_k^{\mathrm{PD}}(\mathrm{t})$ and the output signal at the loop filter (LF, blue) by $x_k^{\mathrm{C}}(\mathrm{t})$.

2. Phase model of mutually delay-coupled phase-locked loops

PLLs are electronic components able to synchronize their clock signals by evaluating mutual phase differences and adjusting frequencies accordingly. A PLL [5, 6] contains three essential building blocks (figure 2): the phase detector (PD), the loop filter (LF) and the voltage-controlled oscillator (VCO) with adjustable frequency and intrinsic frequency ω for zero-controlled voltage. These three components are organized in a loop where the output signal x_k is fed back to the PD (figure 2). A PLL that receives a constant input x_l operates like a free-running oscillator at frequency ω of the VCO. For periodic input signals, the PD yields an output signal $x_k^{\mathrm{PD}}(\mathrm{t})$ with low and high frequency components. The high frequency components are damped by the LF. The low frequency components yield a control signal $x_k^{\mathrm{C}}(\mathrm{t})$ for the VCO that modulates its frequency and results in an entrainment to the input signal's phase and frequency. We now develop a phase model for networks of mutually coupled PLLs. For simplicity, we first show the derivation for two PLLs, and subsequently generalize the result to networks of N coupled PLLs.

2.1. Two mutually coupled phase-locked loops

Throughout our work we consider analogue PLLs, implying signals continuous in time. The VCOs output a sinusoidal signal with constant amplitude, which we set to 1 without loss of generality,

$$x_k(t) = \sin \phi_k(t), \tag{1}$$

where $\phi_k(\mathrm{t})$ denotes the phase of the oscillatory signal and $k = 1{,}2$ indexes the PLLs. The phase detector multiplies an external input signal x_l with the output signal x_k of the VCO. We account for transmission delays between the PLLs by a discrete delay τ of the input signal,

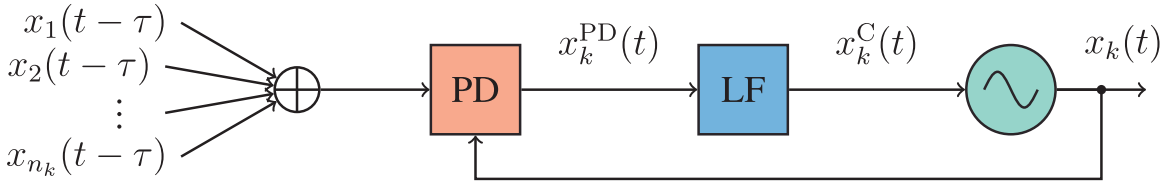

Figure 3. Signal flow of a PLL with N delayed inputs.

$$x_k^{\mathrm{PD}}(t) = x_l(t-\tau)x_k(t) = \frac{1}{2}\cos\Big(\phi_l(t-\tau) - \phi_k(t)\Big) - \frac{1}{2}\cos\Big(\phi_l(t-\tau) + \phi_k(t)\Big), \tag{2}$$

The second identity is obtained using equation (1) and standard trigonometric identities. The signal x_k^{PD} is filtered by the loop filter whose output signal x_k^{C} is given by

$$x_k^{\mathrm{C}}(t) = \int_0^\infty \mathrm{d}u\, p(u) x_k^{\mathrm{PD}}(t-u), \tag{3}$$

where $p(u)$ is the impulse response of the loop filter, which is normalized, $\int_0^\infty \mathrm{d}u\, p(u) = 1$. The output x_k^{C} of the loop filter yields the control signal for the VCO (figure 2). The dynamic frequency of the VCO is given by its intrinsic frequency ω, which is modulated by the control signal x_k^{C},

$$\dot{\phi}_k(t) = \omega + K_{\mathrm{VCO}} x_k^{\mathrm{C}}(t), \tag{4}$$

where K_{VCO} is the sensitivity of the VCO. Since $|x_k^{\mathrm{C}}|$ is of order 1, it can be seen from equation (4) that $|\dot{\phi}_l - \dot{\phi}_k| \leqslant 2K_{\mathrm{VCO}}$ and $|\dot{\phi}_l + \dot{\phi}_k| \geqslant 2(\omega - K_{\mathrm{VCO}})$. Hence, in equation (2), the first term containing a phase difference describes low frequency components of the signal, while the second term containing a sum of phases describes high frequency components. We here consider an ideal loop filter, which perfectly damps these high frequency components. Using equations (2) and (3) in equation (4), we thus find for an ideal loop filter

$$\dot{\phi}_k(t) \simeq \omega + K\int_0^\infty \mathrm{d}u\, p(u) \cos\Big(\phi_l(t-\tau-u) - \phi_k(t-u)\Big), \tag{5}$$

where $K = K_{\mathrm{VCO}}/2$ is the coupling strength. Equation (5) is a closed equation in the phase variables ϕ_{k} for two mutually delay-coupled PLLs.

2.2. Networks of many mutually coupled phase-locked loops

The phase model equation (5) for two mutually coupled PLLs can be straightforwardly extended to a network of N coupled PLLs with identical transmission delays. In this case, each PLL receives multiple input signals, which are combined by a non-inverting adder before being fed into the phase detector (figure 3). The phase model for N coupled PLLs reads

$$\dot{\phi}_k(t) = \omega + \frac{K}{n_k}\sum_{l=1}^{N} c_{kl}\int_0^\infty \mathrm{d}u\, p(u) \cos\Big(\phi_l(t-\tau-u) - \phi_k(t-u)\Big). \tag{6}$$

The connections between PLLs are described by the coupling matrix $\mathbb{C} = (c_{kl})$ with $c_{kl} \in \{0, 1\}$, where $c_{kl} = 1$ indicates a connection between k and l. The coupling strength is

normalized by the number of input signals $n_k = \sum_l c_{kl}$. In general, intrinsic frequencies and transmission delays between PLLs can be inhomogeneous, that is, the intrinsic frequency may depend on the VCO, $\omega = \omega_k$, and the transmission delay may depend on the specific connection, $\tau = \tau_{kl}$. Throughout this paper, we study the case of homogeneous intrinsic frequencies and transmission delays. Equation (6) is an integro-differential equation that describes a network of N coupled PLLs and explicitly includes a filter kernel $p(u)$ and transmission delays τ. The filter kernel describes the damping of different frequency components by the loop filter. For a filter kernel sharply peaked at $u = 0$, $p(u) = \delta(u)$, equation (6) reduces to a Kuramoto model of coupled phase oscillators with transmission delays and cosine coupling function [15–18].

3. Networks of PLLs exhibit synchronized states

Networks of mutually coupled oscillators often tend to synchronize but can also exhibit other complex dynamics. In technical applications, many individual components often need to perform tasks in a concerted way and therefore rely on a common time reference. Such a common time reference can be achieved through global synchronization of all components. Globally in-phase synchronized states are characterized by all oscillators evolving with the same frequency Ω,

$$\phi_k(t) = \Omega t, \tag{7}$$

and exhibiting no phase lag with respect to each other. Substituting equation (7) into equation (6), an algebraic equation for the global frequency Ω can be found,

$$\begin{aligned}\Omega &= \omega + \frac{K}{n_k}\sum_{l=1}^{N} c_{kl}\int_0^\infty \mathrm{d}u\, p(u)\cos(-\Omega\tau)\\ &= \omega + K\cos(\Omega\tau)\end{aligned} \tag{8}$$

where we have used $\int_0^\infty \mathrm{d}u\, p(u) = 1$ and $n_k = \sum_l c_{kl}$. This result is valid for any coupling topology if there is no disjoint set of nodes. Interestingly, for identical PLLs the global frequency Ω does not depend on the parameters of the loop filter and is identical to that of a Kuramoto model with uniform discrete delay and cosine coupling function [18].

4. Stability of synchronized states

Whether a globally synchronized state can be achieved depends on its stability properties, that is, whether perturbations to this state grow or decay.

4.1. Linearization of the dynamics

To determine stability of the in-phase synchronized state for systems of identical PLLs and uniform transmission delays, in equation (7), we perform a linear stability analysis [19, 20]. We use the ansatz

$$\phi_k(t) = \Omega t + \varepsilon q_k(t), \tag{9}$$

where q_k is a perturbation to the in-phase synchronized state, equation (7), and ε is a small expansion parameter. Expanding equation (6) to first order in ε at $\varepsilon = 0$ yields the linear dynamics of the perturbation,

$$\dot{q}_k(t) = \frac{\alpha}{n_k}\sum_{l=1}^{N} c_{kl}\int_0^\infty \mathrm{d}u\, p(u)\Big[q_l(t-\tau-u) - q_k(t-u)\Big] + \mathcal{O}(\varepsilon), \tag{10}$$

where

$$\alpha = K\,\sin(\Omega\tau). \tag{11}$$

Substituting the exponential ansatz $q_k(t) = v_k \mathrm{e}^{\lambda t}$ with $\lambda \in \mathbb{C}$ [19] into equation (10), we obtain the characteristic equation

$$\lambda v_k = \frac{\alpha}{n_k}\hat{p}(\lambda)\sum_{l=1}^{N} c_{kl}\Big(v_l \mathrm{e}^{-\lambda\tau} - v_k\Big), \tag{12}$$

where $\hat{p}(\lambda) = \int_0^\infty \mathrm{d}u\, p(u)\,\mathrm{e}^{-\lambda u}$ is the Laplace transform of the filter kernel $p(u)$. In general, the characteristic equation (12) can have multiple complex solutions λ. The in-phase synchronized state equation (7) is linearly stable if and only if $\mathrm{Re}\,(\lambda) < 0$ for all solutions to equation (12), which implies an exponential decay of small perturbations to the synchronized state. In this case, the solution λ_0 with the largest real part determines the long-time behavior of the decay. The in-phase synchronized state equation (7) is linearly unstable if and only if $\mathrm{Re}\,(\lambda) > 0$ for at least one solution to equation (12), which implies exponential growth of small perturbations to the synchronized state. In this case, the solution λ_0 with the largest real part determines how fast the system deviates from the synchronized state. In both cases, the system is dominated by the solution λ_0 with the largest real part, whose real and imaginary part we denote by

$$\lambda_0 = \sigma + \mathrm{i}\beta, \tag{13}$$

where σ is the perturbation response rate. The imaginary part β is a frequency that modulates the global frequency Ω; see appendix A. Note that β refers to a frequency qualitatively different from the dynamic frequencies of the PLLs.

Note that in the absence of a transmission delay, the synchronized state is only neutrally stable: for $\tau = 0$, equation (11) implies $\alpha = 0$ and equation (12) only permits the solution $\lambda = 0$, so that perturbations neither decay nor grow. This indicates neutral stability, where any small perturbation persists. Hence, non-zero transmission delays are required for stable in-phase synchronized states to exist. This is in contrast to numerous other oscillator systems, in which coupling between oscillators is described by a sine function instead of the cosine function in equation (6) [17, 21, 22]. Hence, two unfavorable effects for in-phase synchronization (cosine coupling and transmission delay) combined yield a desirable effect.

We obtain solutions λ to equation (12) by rewriting equation (12) in vector form

$$\mathrm{e}^{\lambda\tau}\left(\frac{\lambda}{\alpha\hat{p}(\lambda)} + 1\right)\mathbf{v} = \mathbb{D}\mathbf{v}, \tag{14}$$

with $\mathbf{v} = (v_1, \ldots, v_N)$ and the normalized coupling matrix $\mathbb{D} = (d_{kl})$ with $d_{kl} = c_{kl}/n_k$. Clearly, for any solution λ, the scalar coefficient on the lhs of equation (14) is an eigenvalue of $\mathbb{D}$. A strategy to solve equation (14) is thus to solve the equation $\mathrm{e}^{\lambda\tau}(\lambda/\alpha\hat{p}(\lambda) + 1) = \zeta$ for each eigenvalue ζ of $\mathbb{D}$. The corresponding eigenvectors $\mathbf{v}$ are collective perturbation modes for which the linearised dynamics decouples.

4.2. Description of the loop filter

For a large class of loop filters, the filter kernel is given by

$$p(u) = u^{a-1}\frac{\mathrm{e}^{-u/b}}{b^a \Gamma(a)}, \tag{15}$$

where a corresponds to the order of the loop filter and b determines the cut-off frequency ω_c according to $\omega_c = (ab)^{-1}$ [23]. The functional form equation (15) corresponds to the Gamma distribution in statistics. The Laplace transform of the filter kernel entering the characteristic equation (14) is given by

$$\hat{p}(\lambda) = \int_0^\infty \mathrm{d}u\, p(u)\mathrm{e}^{-\lambda u} = \frac{1}{(1+\lambda b)^a}. \tag{16}$$

Substituting into equation (14), we find the characteristic equation

$$\lambda(1+\lambda b)^a + \alpha\left(1 - \zeta \mathrm{e}^{-\lambda\tau}\right) = 0. \tag{17}$$

Note that for each eigenvalue ζ this equation can have multiple solutions in λ. For $|\lambda| \ll 1$ we can expand equation (17) in λ and obtain

$$\sum_{m=0}^{M} \chi_m \lambda^m = 0, \tag{18}$$

where M denotes the order of expansion and the first four expansion coefficients χ_m are given by $\chi_0 = \alpha(1-\zeta)$, $\chi_1 = 1 + \alpha\tau\zeta$, $\chi_2 = ab - \alpha\tau\zeta/2$, and $\chi_3 = (ab^2/2)(a - 1 + \alpha\tau^3\zeta/3)$. Note that the approximation equation (18) can be solved in closed form up to order $M \leqslant 3$ and thus permits analytical solutions, while equation (17) has to be solved numerically.

5. Specific PLL networks as examples

Using specific examples, we now show that our phase model is able to describe the key features of synchronization in systems of delay-coupled PLLs. To this end, we compare analytical solutions of the phase model equation (6) to results obtained from MATLAB/Simulink simulations. MATLAB/Simulink simulates the separate PLL components and the wire-induced delays. In contrast to our idealized description of the loop filter, MATLAB/Simulink does not assume perfect damping of high frequency components. Hence, these more detailed simulations provide a test of whether the phase model equation (6) can quantitatively capture the dynamics of a network of delay-coupled PLLs. In the following, we present two simple examples of networks of mutually delay-coupled identical PLLs: a system with $N = 2$ coupled PLLs and a 3×3 square lattice of nearest-neighbor coupled PLLs ($N = 9$) with periodic boundary conditions, see figure 4.

5.1. Collective frequency of the synchronized states

For technical applications, the specific frequency at which the system operates is a key property for its intended purpose. Whether a specific global frequency can be achieved depends on the system specifications. We here find that the collective frequency of the in-phase synchronized state, equation (8), depends on the intrinsic frequency of the VCOs, the coupling strength, and

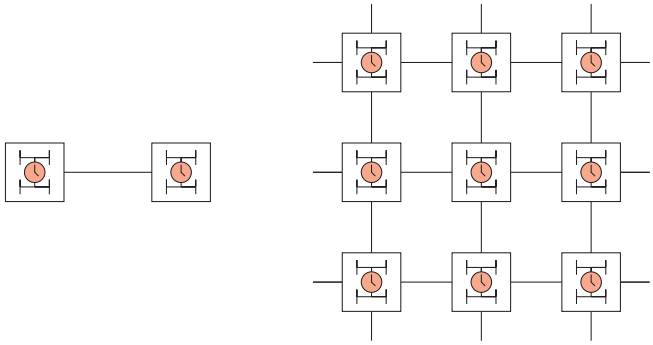

Figure 4. Left: two mutually coupled PLLs. Right: 3 × 3 lattice of $N = 9$ mutually coupled PLLs with periodic boundary conditions.

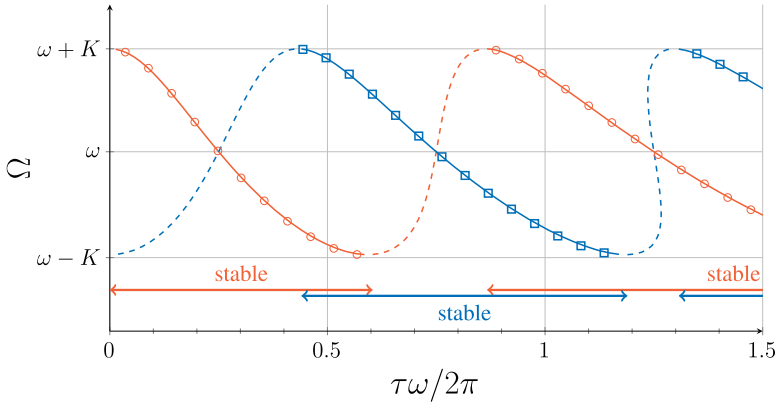

Figure 5. Global frequency Ω of the in-phase (orange) and anti-phase (blue) synchronized state for $N = 2$ mutually coupled PLLs as a function of the transmission delay τ. Lines show analytical results of the phase model, equation (8), where solid lines denote stable solutions and dashed lines denote unstable solutions (see section 4). Symbols denote numerical results from MATLAB/Simulink simulations.

the coupling delay. However, it is independent of the number of PLLs, the coupling topology, and the properties of the loop filter. Simulating the system of $N = 2$ PLLs for different values of the transmission delay and for different initial conditions using MATLAB/Simulink (see appendix B), we find (i) the in-phase synchronized state discussed in section 3, and (ii) an anti-phase synchronized state, characterized by $\phi_1(t) = \phi_2(t) - \pi$. The system considered here exhibits bistability of both solutions in certain regions in parameter space. To obtain the frequency of both solutions in simulations, the system has to be prepared in different initial conditions.

The lines in figure 5 display the collective frequency of the synchronized states as obtained from the phase model, equation (8), as a function of the transmission delay τ for the parameters given in table 1. The collective frequency of the anti-phase state can be obtained equivalently as $\Omega = \omega - K \cos(\Omega\tau)$; note the inverted sign compared to equation (8). The symbols in figure 5 show the results of MATLAB/Simulink simulations. We find excellent agreement between these simulations and our analytical results. Depending on the value of the delay, either only one solution or multiple solutions are stable, as shown in the next section.

Table 1. System parameters of the example.

Parameter	Value
VCO free running frequency ω	$2\pi \cdot 3.55$ GHz
Coupling strength K	$2\pi \cdot 1.11$ GHz
LF order a	1
LF cut-off frequency $\omega_c = (ab)^{-1}$	$2\pi \cdot 355$ MHz

5.2. Dynamics of synchronization

Besides the frequency of operation, the time scale at which clocking systems achieve synchrony is crucial for their technical applicability. For small perturbations to synchronized states, this time scale is determined by the perturbation response rate σ (section 4). We compare the response rates obtained from our phase model, equation (13), with results from MATLAB/Simulink simulations (see appendix C for details).

In section 4, we found that the response rates depend on the coupling topology through the eigenvalues ζ of the coupling matrix $\mathbb{D}$. For the two systems considered here, the eigenvalues ζ are given by 1 and -1 for the system of $N = 2$ mutually coupled PLLs and by 1, $-1/2$, and $1/4$ for the 3×3 square lattice of nearest-neighbor coupled PLLs with periodic boundary conditions. In both cases, the eigenvalue 1 corresponds to a collective perturbation mode that shifts the phases of all oscillators by the same amount. Numerically, we find that the perturbation response rate of this global phase shift is always $\sigma = 0$, that is, perturbations neither grow nor decay. Hence, we neglect this neutrally stable perturbation mode in our considerations. The remaining set of eigenvalues is different for both examples, which therefore have to be studied separately.

In particular, the response rates depend on the transmission delay and the properties of the loop filter. We now study these dependencies in the system of $N = 2$ PLLs. For this example, the eigenvalue -1 corresponds to a collective perturbation mode representing the phase difference between the oscillators. The results for the perturbation response rate as a function of the transmission delay are plotted in figure 6, comparing the results from the phase model, equation (13), with those from MATLAB/Simulink simulations. Both results are in very good quantitative agreement. We find that the transmission delay determines whether the in-phase synchronized state is stable or not. Such behavior is consistent with previous studies of different coupled oscillator systems with delays [18]. Furthermore, the synchronization rate is a non-monotonic function of the transmission delay and exhibits local extrema corresponding to a fast decay of perturbations.

We study the effects of filtering on the perturbation response rates by varying the cutoff frequency ω_c of the filter (figure 7). For small cutoff frequencies ($\omega_c < \omega$), the results of MATLAB/Simulink simulations are in excellent quantitative agreement with the result from the phase model For high cutoff frequencies ($\omega_c > \omega$), the results of MATLAB/Simulink simulations deviate quantitatively from those of the phase model as the approximation of an ideal loop filter becomes less accurate. We find that smaller cutoff frequencies tend to cause slower synchronization and lead to a more inert control behavior. It follows that the cutoff frequency of the loop filter can be used to optimize between fast synchronization or strong suppression of high-frequency components.

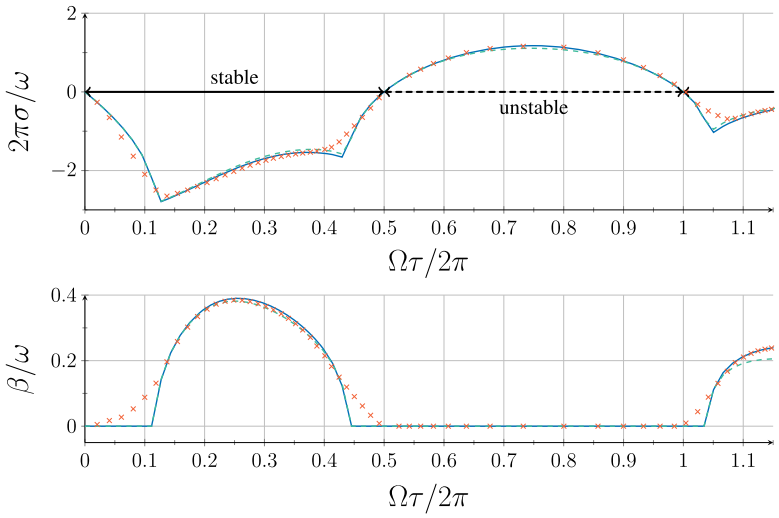

Figure 6. Perturbation response rate σ and corresponding modulation frequency β as a function of the transmission delay for a system of $N = 2$ mutually coupled PLLs. Numerical solution to the characteristic equation (17) for λ (solid blue), approximate analytic solution equation (18) (dashed green), and results obtained from MATLAB/ Simulink simulations (red symbols). Parameters are given in table 1.

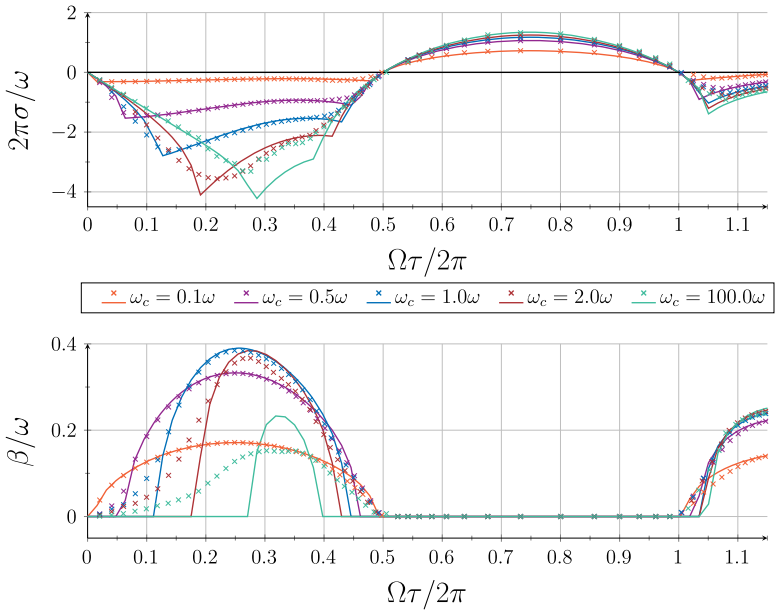

Figure 7. Perturbation response rate σ and corresponding modulation frequency β as a function of the transmission delay for a system of $N = 2$ mutually coupled PLLs for different cutoff frequencies (see legend). Numerical solution to the characteristic equation (17) (curves) and results obtained from MATLAB/Simulink simulations (symbols). Other parameters are given in table 1.

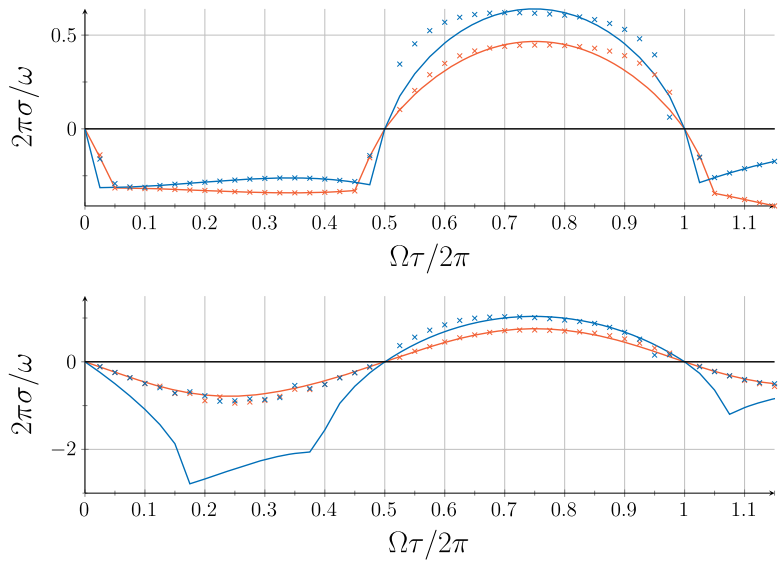

Figure 8. Perturbation response rate σ as a function of the transmission delay for a 3×3 square lattice of nearest-neighbor coupled PLLs with periodic boundary conditions for the filter cutoff frequencies $\omega_c = 0.1\omega$ (upper plot) and $\omega_c = \omega$ (lower plot). Numerical solution to the characteristic equation (17) (curves) and results obtained from MATLAB/Simulink simulations (symbols). Different colors correspond to different perturbation modes with eigenvalues 1/4 (orange) and $-1/2$ (blue).

In the system of $N = 2$ mutually coupled PLLs, only one non-trivial perturbation mode exists. To study the behavior of different perturbation modes, we now consider the system of a 3×3 square lattice of nearest-neighbor coupled PLLs with periodic boundary conditions. This system has two non-trivial perturbation modes, corresponding to the eigenvalues $-1/2$ and $1/4$ of the coupling matrix. To compare the results of our phase model with those of MATLAB/Simulink simulations, we excite these two perturbation modes individually and measure the perturbation response rate (see appendix C). In figure 8, we display the perturbation response rates as a function of the transmission delay for both perturbation modes and two different cutoff frequencies. For small cutoff frequencies (upper plot), we again find very good agreement between results from MATLAB/Simulink simulations and the phase model. For cutoff frequencies comparable to the intrinsic frequency of the VCO (lower plot), in simulations only one synchronization rate is observed for a specific transmission delay in the stable regimes. This behavior signals the breakdown of the ideal loop filter approximation in the phase model (see appendix C).

6. Discussion

In this paper, we have studied synchronization in networks of mutually delay-coupled identical PLLs using a general phase oscillator description. Our theory captures the properties of filters in the PLLs as well as the effects of uniform transmission delays. We showed that transmission delays play a crucial role for synchronization. Undelayed coupling between PLLs does not reduce mutual phase differences. In contrast, transmission delays affect phase differences and can lead to stable in-phase or anti-phase synchronization. Thus, unavoidable delays that occur at

high clock rates can play a constructive role in network synchronization. The time scales at which the system reaches such a globally synchronized state are determined by the effects of filtering and transmission delays. The global frequency of the synchronized network in general differs from the intrinsic frequency of the PLLs and depends on the system specifications. We have shown that our phase description can quantitatively account for the behavior of PLL networks using detailed simulations of components in MATLAB/Simulink.

Real systems of coupled PLLs can exhibit a variability in the intrinsic frequencies and transmission delays. In general, small variability in the intrinsic frequencies and/or transmission delays can still permit reliable synchronization provided that the coupling is strong enough [17, 24, 25]. Large variability in the frequencies and delays could lead to qualitatively different behaviors such as phase-lag synchrony or incoherent states [17, 24]. In this paper, we focused on the case of identical PLLs and uniform transmission delays which allowed us to study the key principles in a simplified scenario. How strong variability in frequencies and delays will affect synchronization in systems of coupled PLLs will be subject of future research.

For technical implementations of clocking networks, fast and robust synchronization and a tunable frequency at low energy consumption are key requirements. Our results suggest that a square lattice of mutually delay-coupled PLLs with nearest-neighbor coupling could be a way to achieve these goals. Such an architecture is simple to implement, highly scalable, and limits energetic costs of signal amplification, as it only requires short wiring distances. Furthermore, our results show that transmission delay and filter characteristics are among the major factors determining the synchronization properties of the network and hence are important design parameters. These can be tuned by, e.g., introducing additional delay components in the connections or adjusting the response of the filter components. Our theory provides a practical tool to determine the specific system parameters needed for robust synchronization. Large lattices of mutually delay-coupled PLLs might exhibit other dynamical states in addition to the in-phase synchronized states. One possibility to ensure that the system reaches an in-phase synchronized state is to sequentially couple additional PLLs to an already synchronized smaller network, thereby growing the network stepwise until the system is globally synchronized. This and other strategies to reach globally in-phase synchronized states will be an interesting and important topic for further research.

Acknowledgements

We thank Saúl Ares and Luis Morelli for stimulating discussions about phase oscillators. This work is partly supported by the German Research Foundation (DFG) within the Cluster of Excellence ‘Center for Advancing Electronics Dresden’.

Appendix A. Modulation of global frequency in transient dynamics

As perturbations to the synchronised states decay, the perturbation response may modulate the global frequency as given by the modulation frequency β. Close to the in-phase synchronized state, the phase of oscillator k is given by equation (9) with $q_k(t) = v_k e^{\sigma t} \cos(\beta t)$. For small perturbations, $\varepsilon \ll 1$, the VCO output signal, equation (1), is given by

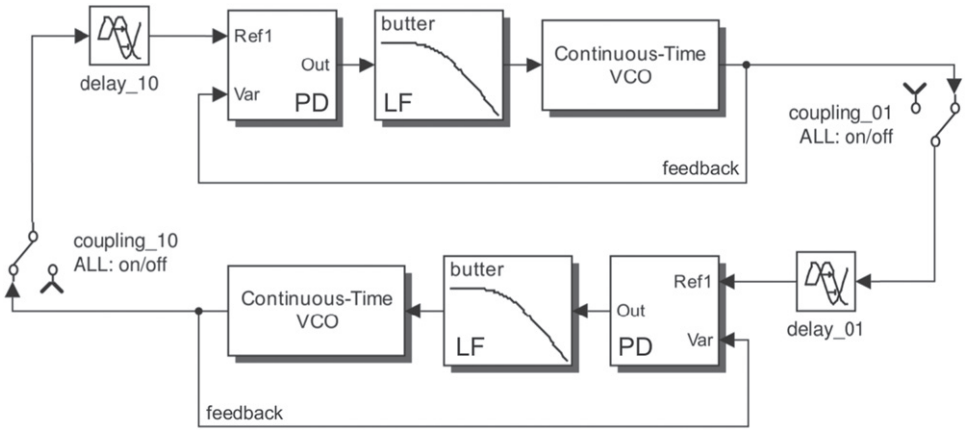

Figure B1. Circuit diagram of two mutually delay-coupled phase locked loops taken from MATLAB/Simulink [26]. For the loop filter (LF) `butter` denotes the Butterworth filter design of the LF. The phase detector (PD) receives two inputs, the delayed signal of the other PLL via channel `Ref1` and the feedback signal via channel `Var`.

$$\begin{aligned} x_k(t) &= \sin\left(\Omega t + \varepsilon v_k \cos(\beta t) e^{\sigma t}\right) \\ &= \sin(\Omega t) + \varepsilon v_k \cos(\Omega t)\cos(\beta t) e^{\sigma t} + \mathcal{O}(\varepsilon^2) \\ &= \sin(\Omega t) + \frac{\varepsilon}{2} v_k e^{\sigma t}(\cos([\Omega + \beta]t) + \cos([\Omega - \beta]t)) + \mathcal{O}(\varepsilon^2). \quad \text{(A.1)} \end{aligned}$$

In addition to the global frequency Ω two side-bands in the frequency domain $\Omega \pm \beta$ exist. These side-bands decay with rate σ as the perturbation to the synchronized state decays.

Appendix B. Identification of phase-model parameters with Matlab/Simulink simulation parameters

MATLAB/Simulink provides a library of virtual electronic components, so called blocks, that can be interconnected using a graphical user interface. The dynamics of the resulting systems are simulated and the time evolution of the signals can be monitored anywhere in the circuit. For our simulations we used four types of blocks: phase detector blocks (PD), loop filter blocks (LF), time-continuous voltage-controlled oscillator blocks (VCO), and transport-delay blocks (delay), see figure B1 . The PD block performs a multiplication of its input signals. For the LF block, we chose the butterworth design option with a filter order of one and a passband edge frequency equal to the cut-off frequency in our phase model. Since the other frequencies in MATLAB/Simulink are not angular frequencies, we have to transform the angular frequencies used in our phase model accordingly. The time-continuous VCO is characterized by a voltage signal output amplitude that we set to 1 V and a quiescent frequency $f_\omega = \omega/2\pi$ corresponding to the intrinsic frequency ω of our phase model. The input sensitivity K_{VCO} is the frequency change per unit voltage in response to the input signal of the VCO. It is related to the coupling strength K in the phase model by $K_{\mathrm{VCO}} = 2 \times K/2\pi$. These blocks are connected to form PLLs that are mutually coupled. Transport-delay blocks are placed at the interconnections between the PLLs with a time delay equivalent to the transmission delay τ in our phase model. The initial

output for $t \leqslant \tau$ of the transport-delay blocks were set to an oscillatory signal with the intrinsic frequency of the VCOs.

Appendix C. Determining perturbation response rates from MATLAB/Simulink simulations

Here we describe how we measure synchronization rates of different perturbation modes in MATLAB/Simulink simulations. The description of the VCO in these simulations can be considered as the solution to an amplitude model studied in reference [27]. These simulations yield an analytic VCO signal that makes it straightforward to extract the phase signal.

We start the system in the in-phase synchronized state and add small perturbations to measure their decay rate. If these perturbations are chosen randomly, in general all perturbation modes are excited. Since each mode has a different decay rate, the mode with the slowest rate governs the long-time behavior of synchronization. To obtain this slowest decay rate, we compute the Kuramoto order parameter [16]

$$R(t)\mathrm{e}^{\mathrm{i}\psi(t)} = \frac{1}{N}\sum_{k=1}^{N}\mathrm{e}^{\mathrm{i}\phi_k(t)} \tag{C.1}$$

as a function of time. As the system synchronizes, the magnitude $R(t)$ approaches unity. The long-time behavior of $R(t)$ is given by the slowest decaying mode, $1 - R(t) \sim \mathrm{e}^{\sigma t}\cos(\beta t)$, where σ is the perturbation response rate and β is the modulation frequency [28]. Hence, σ and β can be obtained by fitting the magnitude $R(t)$ of the order parameter. The results are shown in figures 6 and 7.

The synchronization rate of the faster decaying modes can be accessed by exciting specific eigenmodes of the system exclusively and using the same analysis. To obtain the data shown in figure 8, we have used the eigenmodes of the phase model, which we can compute explicitly (section 4), to perturb the system. In the case of figure 8, this procedure provides a faster relaxation time corresponding to a second mode. Using the eigenmodes of the phase model to perturb MATLAB/Simulink simulations works as long as higher frequency components are suppressed. This condition is not satisfied in the second case, shown in figure 8, where the analytic eigenmodes of the phase model are not accurate enough and therefore other modes including the slowest are excited. Therefore, the slowest perturbation response rate dominates the relaxation dynamics.

References

[1] Ramacher U 2007 *Computer* **40** 62–69
[2] Wolf W, Jerraya A A and Martin G 2008 *IEEE Trans. Comput.-Aided Des. Integr. Circuits* **27** 1701–13
[3] Bjerregaard T and Mahadevan S 2006 *ACM Comput. Surveys (CSUR)* **38** 1
[4] Benini L and de Micheli G 2002 *Computer* **35** 70–78
[5] Gardner F M 2005 *Phaselock Techniques* (New York: Wiley)
[6] Meyr H and Ascheid G 1990 *Synchronization in digital communications: Phase-, frequency-locked loops and Amplitude Control* vol 1 (New York: Wiley)
[7] Ho R, Mai K and Horowitz M 2001 *Proc. IEEE* **89** 490–504
[8] Mensink E, Schinkel D, Klumperink E, van Tuijl E and Nauta B 2010 *IEEE J. Solid-State Circuits* **45** 447–57

[9] Yu Z and Baas B 2009 *IEEE Trans. Very Large Scale Integr. Syst.* **17** 66–79
[10] Semeraro G, Magklis G, Balasubramonian R, Albonesi D, Dwarkadas S and Scott M 2002 Energy-efficient processor design using multiple clock domains with dynamic voltage and frequency scaling *Proc. 8th Int. Symp. on High-Performance Computer Architecture* pp 29–40
[11] Ginosar R 2003 Fourteen ways to fool your synchronizer *Proc. 9th Int. Symp. on Asynchronous Circuits and Systems* pp 89–96
[12] Lindsey W C, Ghazvinian F, Hagmann W C and Dessouky K 1985 *Proc. IEEE* **73** 1445–67
[13] Javidan M, Zianbetov E, Anceau F, Galayko D, Korniienko A, Colinet E, Scorletti G, Akre J M and Juillard J 2011 All-digital PLL array provides reliable distributed clock for SOCs *IEEE Int. Symp. on Circuits and Systems* pp 2589–92
[14] Orsatti F M, Carareto R and Piqueira J R C 2008 *IET Circuits Dev. Syst.* **2** 495–508
[15] Kuramoto Y 1975 Self-entrainment of a population of coupled non-linear oscillators *Int. Symp. on Mathematical Problems in Theoretical Physics* (*Lecture Notes in Physics* vol 39) ed H Araki (Berlin: Springer) pp 420–2
[16] Kuramoto Y 1984 *Chemical Oscillations, Waves, and Turbulence* (Berlin: Springer)
[17] Yeung M K S and Strogatz S H 1999 *Phys. Rev. Lett.* **82** 648–51
[18] Earl M G and Strogatz S H 2003 *Phys. Rev.* E **67** 036204
[19] Strogatz S H 2008 *Nonlinear Dynamics And Chaos: With Applications to Physics Biology Chemistry and Engineering* (Reading, MA: Perseus Books)
[20] Amann A, Schöll E and Just W 2007 *Physica* A **373** 191–202
[21] Acebrón J A, Bonilla L L and Vicente C J P 2005 *Phys. Mod. Rev.* **77** 137–85
[22] Schuster H G and Wagner P 1989 *Prog. Theor. Phys.* **81** 939–45
[23] Mancini R C 2003 *Op Amps For Everyone: Design Reference* 2nd edn (London: Newnes)
[24] Strogatz S H 2000 *Physica* D **143** 1–20
[25] Papachristodoulou A and Jadbabaie A 2006 Synchonization in oscillator networks with heterogeneous delays, switching topologies and nonlinear dynamics *45th IEEE Conf. on Decision and Control* pp 4307–12
[26] MATLAB 2013 *2013a* (Natick, MA: The MathWorks Inc.)
[27] Chen Y and Scholtz R A 2005 A theoretical model of a voltage controlled oscillator *Record of the 39th Asilomar Conf. on Signals, Systems and Computers* pp 1114–8
[28] Wetzel L 2012 Effect of distributed delays in systems of coupled phase oscillators *PhD Thesis* TU Dresden